Journal of
Materials Chemistry B

COMMUNICATION

View Article Online
View Journal

Cite this: DOI: 10.1039/c6tb02198k

Received 27th August 2016,
Accepted 22nd March 2017

DOI: 10.1039/c6tb02198k

rsc.li/materials-b

Reprogrammable ultra-fast shape-transformation of macroporous composite hydrogel sheets†

Hongyu Guo,‡[a] Jian Cheng,‡[b] Jianying Wang,[a] Peng Huang,[c] Yijing Liu,[d] Zheng Jia,[b] Xiaoyuan Chen,[d] Kunyan Sui,*[e] Teng Li*[b] and Zhihong Nie*[a]

In this communication, we report a composite macroporous hydrogel sheet that can rapidly transform into multiple 3D shapes in response to near-infrared (NIR) light on demand. The transformation relies on the photo-thermal-induced asymmetric shrinking of the hydrogel material, which is further verified by finite element modeling.

Nature is replete with self-adaptive phenomena. Examples include humidity-mediated opening of plant organs, leaf wrinkling, tendril coiling, Venus flytrap, *etc.*[1–4] Inspired by nature, researchers have made great efforts to design and fabricate adaptive polymeric hydrogel materials that are capable of transforming in response to environmental stimuli, such as temperature, pH, ions, electricity, humidity, external field and light, to name a few.[5,6] Self-shaping hydrogel materials have found a wide range of applications such as in soft robotics, artificial muscles, biomedicine, microfluidics, actuators, *etc.*[6–8] Generally, a stimuli-induced differential swelling within the hydrogel is required for it to bend, twist and fold.[6] As an example, a hydrogel sheet with a bilayer structure can bend upon temperature change due to the mismatch in the extent of swelling between the two layers.[9,11,12] Among various environmental stimuli, light is particularly attractive as it can be implemented without contacting the material and can be remotely controlled.[10,13,14] Light has been used to actuate liquid crystal films,[15–17] bend reduced–graphene–oxide–elastin composites,[10] and transform polymer–inorganic hybrid networks[18] and carbon-nanotube-doped polymer films,[13,19] *etc.*

It is truly amazing that in nature octopuses can transform to adapt almost arbitrary shapes in order to survive.[20] The ability to mimic octopus's morphing strategy and design of self-shaping hydrogel materials that are capable of transforming into rich shapes are needed. At present, most self-shaping hydrogel materials are designed to acquire one or few specific pre-determined shapes through preprogrammed shape transformations in response to external stimuli.[21–24] In this case, one or more responsive components are patterned in the hydrogel sheet and the types of target shapes are often predetermined at the stage of patterning. Kumacheva and coworkers recently reported that the same hydrogel sheet patterned with multiple responsive components can be transformed into three different shapes upon exposure to different stimuli.[25] The accessible shape transformations of the pre-patterned hydrogel, however, are restricted by the limited number of responsive components that can be integrated into the sheet and the interference between these components in response to a specific stimulus. Recently, Hayward *et al.* demonstrated that the shape transformation of light-responsive composite hydrogels can be modulated to produce multiple shapes by controlling light irradiation patterns.[26] It is striking that the configurations that can be achieved from the same piece of these hydrogel sheets are infinite in theory. In their work, a characteristic response time of $\tau \approx 2$–3 s was found for their composite hydrogel with a thickness of 25 μm. However, since the gel shape-transforming rate (τ) increases quadratically with the thickness (h_0) of the hydrogel film as $\tau \sim h_0^2$, the transformation of a thicker hydrogel sheet would be rather slow. As an example, it would take up to fifteen minutes to reach an equilibrium state in shape when the thickness is approximately 500 μm.[26] Previous studies suggest that introducing pores within self-shaping hydrogels can greatly increase the shape-transforming rate of hydrogels due to enhanced mass transport.[9,10] However, to date a fast on-demand transforming hydrogel with macropores has never been demonstrated.

[a] *Department of Chemistry and Biochemistry, University of Maryland, College Park, MD, 20742, USA. E-mail: znie@umd.edu*
[b] *Department of Mechanical Engineering, University of Maryland, College Park, MD, 20742, USA. E-mail: LiT@umd.edu*
[c] *Guangdong Key Laboratory for Biomedical Measurements and Ultrasound Imaging, School of Biomedical Engineering, Shenzhen University, Shenzhen, 518060, P. R. China*
[d] *Laboratory of Molecular Imaging and Nanomedicine (LOMIN), National Institute of Biomedical Imaging and Bioengineering (NIBIB), National Institutes of Health, USA*
[e] *Department of Polymer Science and Engineering, State Key Laboratory Cultivating Base for New Fiber Materials and Modern Textiles, Qingdao University, Qingdao, China. E-mail: kunyansui@163.com*

† Electronic supplementary information (ESI) available. See DOI: 10.1039/c6tb02198k

‡ These authors contributed equally to this work.

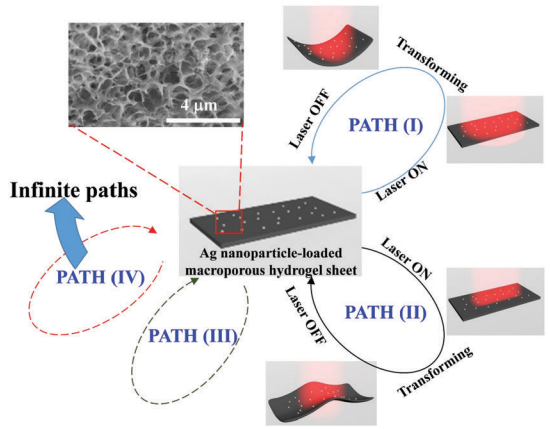

Scheme 1 Schematic illustration of a hybrid hydrogel sheet that can transform into different geometries in response to near-infrared (NIR) light. The hybrid hydrogel sheet consists of a macroporous PNIPAM hydrogel embedded with silver nanoparticles (AgNPs) capable of converting absorbed light into heat. When subjected to NIR laser irradiation with different patterns, the same hydrogel sheet can transform into different geometries; and it recovers its original flat shape when the laser is off. The SEM image in the inset shows the macroporous feature of the hydrogel sheet.

Here we report the design of a macroporous hybrid hydrogel sheet that can undergo an ultra-fast shape transformation and acquire at least five (unlimited number in theory) well-defined geometric configurations in response to near-infrared (NIR) light (Scheme 1). The macroporous hybrid hydrogel sheet is composed of a thermo-responsive polymer, poly(*N*-isopropyl acrylamide) (PNIPAM), embedded with silver nanoparticles (AgNPs) that are capable of converting absorbed light to heat (so-called photothermal effect). Both our experimental and computational studies showed that the light-triggered shape transformation arises from the combination effect of the photothermal heating of AgNPs and thermo-responsiveness of PNIPAM. The representative shapes obtained from the same hydrogel sheet include helical, boat-like, hoof-like, and saddle-like structures. The presence of macropores in the sheet significantly enhanced the transport of water molecules when it underwent swelling or shrinkage,[27] thus enabling the rapid reversible shape transformation of the hydrogel sheet. The shape transformations reached maximum on the order of seconds while it usually takes minutes or even hours for a macroscale nonporous hydrogel of similar thickness to reach its maximum transformation.[25] There are several important features of the design, which distinguish this work from others, including: (i) the hydrogel bears macropores and hence the shape transformation is extremely fast; (ii) the hydrogel material is reprogrammable and multiple well-defined shape transformations (at least five) are obtained from the same 2-D sheet; (iii) light as a stimulus can be remotely controlled; (iv) NIR light is less harmful than UV and visible light, and has a larger penetration depth in biological tissues.

To fabricate the macroporous hybrid hydrogel sheet, poly(ethylene glycol) (PEG), a pore-forming reagent (Fig. S1, ESI†), was added to the hydrogel precursor composed of *N*-isopropyl acrylamide (monomer), *N*,*N*′-methylenebisacrylamide (cross-linker), 2-hydroxy-2-methylpropiophenone (photo-initiator) and water. Subsequent UV photopolymerization and removal of PEG by washing produced hydrogel sheets with macroporous structures (Fig. S3, ESI†). The size of the pores is estimated to be in the range of 200 nm to 1 μm (Fig. S3, ESI†). AgNPs were integrated within the PNIPAM hydrogel sheet by *in situ* reduction of silver nitrate (Fig. S4, ESI†). The as-synthesized AgNPs in the hydrogel sheet showed a roughly spherical shape and a broad size distribution (Fig. S13, ESI†). Under the current experimental conditions, the AgNP-loaded hydrogel showed a fairly strong absorption at 808 nm wavelength, though its absorption peak located at around 595 nm (see Fig. S2, ESI†). The red-shift of the absorption peak of spherical AgNPs from around 400 nm can be attributed to the dense packing of AgNPs in the hydrogel, as indicated by the dark, shining and non-transparent appearance of the gel (Fig. S4, ESI†). A continuous-wave NIR laser (wavelength: 808 nm) was used to trigger the transformation of the hydrogel sheet into different shapes.

By simply tuning the NIR light irradiation pattern on the same sheet, the hybrid sheet can transform into various well-defined shapes, such as boat-like, helical, hoof-like, and saddle-like structures (Fig. 1 and see supporting videos SV1–SV4, ESI†). Upon the removal of light irradiation, the hybrid sheet was able to return to its original flat state and transform into another shape upon light irradiation with a different pattern. All the shape transformations were highly reversible and could be repeated for many cycles (Fig. S18, ESI†). The shape transformations were verified by finite element modeling (Fig. 1b and see supporting videos SV5–SV9, ESI†). The shape transformations are extremely fast (see supporting video SV4, ESI†): upon light irradiation, the macroporous hybrid sheet reaches its transformation maximum on the order of seconds while it usually takes minutes/hours for a macroscale nonporous hydrogel of similar thickness to transform to its maximum.[25] To quantify the behavior of the light-responsive shape-transformation system, we investigated the simple bending deformation of the hybrid sheet upon irradiation with a single striped light pattern. We found that the bending angle increased with the increase in

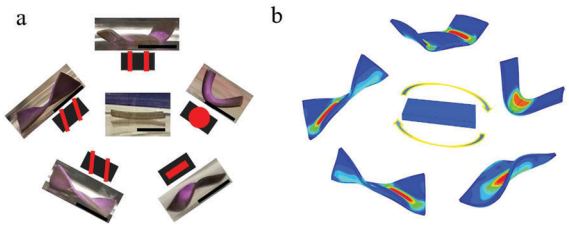

Fig. 1 Experimental (a) and finite element modelling (FEM) (b) results of shape transformations of the same hybrid hydrogel sheet into five different shapes upon NIR light irradiation: boat-like, hoof-like, saddle-like, right-helical and left-helical shapes (from top along the clockwise direction). The red stripes in (a) indicate the shape of the NIR light spot. Scale bar: 0.85 cm. (b) FEM analyses showed that a unique localized stress field was established within the hybrid sheet upon each irradiation, resulting in a specific shape transformation. The red and blue colors in (b) represent high and low stress within the hydrogel, respectively.

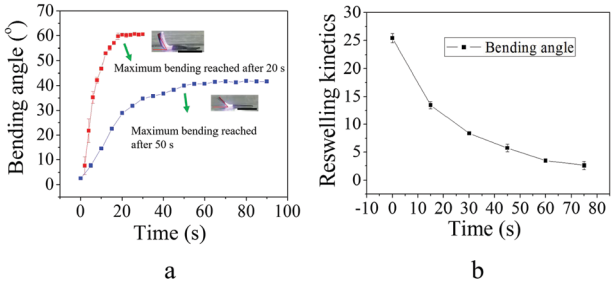

Fig. 2 (a) Bending angle of the composite sheet as a function of irradiation time at different laser power densities. The data points were obtained by averaging the bending angles from three separate cycles. The composite sheet was irradiated at the same position with a rectangular light stripe (width: 0.3 cm) in all the cycles. (b) Re-swelling kinetics of the composite sheet by measuring the time-dependent decrease in bending angle after switching off the laser. The hybrid sheet was irradiated for 5 seconds at a laser power density of 0.94 W cm^{-2}. Then the laser was switched off (corresponding to the data point at 0 second in the graph) and the bending angle was monitored as a function of time.

irradiation time and finally reached a stable bending state (Fig. 2a). The bending rate and time to reach the maximum curvature were strongly dependent on the laser power density. A higher laser power density made the hybrid sheet bend faster as indicated by the larger slope in the red curve (laser power density: 0.94 W cm^{-2}) as compared with the slope in the blue curve (laser power density: 0.57 W cm^{-2}) (Fig. 2a). A higher laser power density also made the sheet reach its maximum bending in a shorter time. It took about 20 seconds for the sheet to bend to its maximum at a laser power density of 0.94 W cm^{-2} (red curve), while it took about 50 seconds at a laser power density of 0.57 W cm^{-2} (blue curve) (Fig. 2a). In addition, the bending angle increased linearly with the increase in laser power density (Fig. 3) and decreased gradually to its original state as a function of time after the laser was switched off (Fig. 2b).

The underlying mechanism of the shape transformation of the macroporous composite hydrogel sheets can be understood as follows. The thermo-responsive polymer, PNIPAM, undergoes a coil-to-globule transition in its aqueous solution when the temperature is above its lower critical solution temperature (LCST) (~32 °C).[28] This transition will result in a volumetric contraction in its hydrogel form due to the expulsion of water molecules.[29] When the hybrid PNIPAM hydrogel was regionally exposed to NIR laser irradiation, the temperature of the irradiated region of the hydrogel increased, while the off-exposure areas remained at a lower temperature. In other words, a non-uniform temperature field was established in the hydrogel under localized light irradiation. As shown in the thermogram (Fig. S6a, ESI†), a remarkable thermal gradient (ranging from 22 °C to 32 °C) was created along the sheet's surface when the sheet was locally irradiated with NIR light. During the irradiation, the thermal gradient on the sheet's surface gradually propagated with the increase of the irradiation time. In addition, the heat propagation occurred also along the thickness direction due to the heat flux input on the laser-exposed area and the convectional dissipation over the other surfaces. This phenomenon was confirmed by the presence of a *z*-direction thermal gradient in the cross-section temperature profile from the simulation (Fig. 4a).

As discussed above, there exist two types of temperature gradients in the hybrid sheet under localized light irradiation: the in-plane thermal gradient and *z*-direction thermal gradient (Fig. 4a). These temperature gradients lead to swelling and modulus differences inside the hydrogel: the regions with higher temperature shrink more and become stiffer (Fig. S11, ESI†). For the bending shape transformation, the in-plane temperature gradient determines the position of the localized deformation, as the bending tip resides at the center of the in-plane gradient. In contrast, the *z*-direction thermal gradient causes a larger volumetric change closer to the top-surface, thus breaking the deformation symmetry along the direction of hydrogel thickness and determining the bending direction. For more complicated shape transformations (saddle, helix, and boat in Fig. 1a), each NIR light illumination generates a signature temperature field inside the hydrogel body, and the interplay of the in-plane and *z*-direction thermal gradient contributes to a unique shape transformation. A real-time temperature evolution and

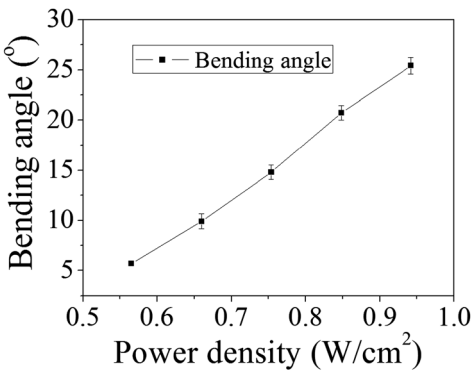

Fig. 3 Bending angle of the composite sheet as a function of laser power density. The composite sheet was irradiated at the same position for 5 seconds at each laser power density using a rectangular laser spot.

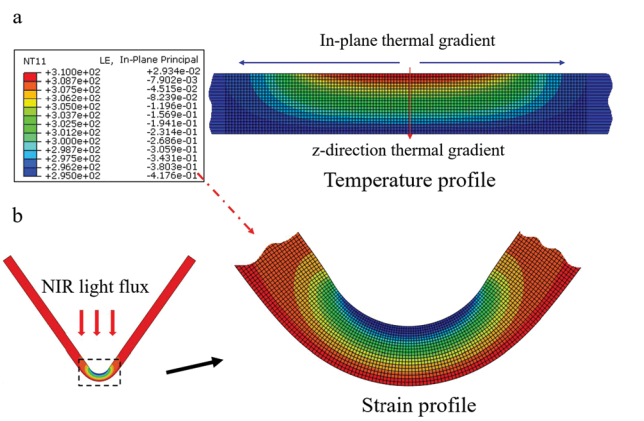

Fig. 4 (a) FEM analysis of temperature distribution within the hybrid sheet upon light irradiation. An infinite convection boundary condition was used in the calculation of the temperature profile. (b) FEM analysis revealed that an asymmetric strain distribution was established within the sheet upon localized light exposure, which essentially actuated the sheet's bending.

the corresponding shape transformation are shown in the supporting videos SV10 and SV11 (ESI†). During the establishment of the thermal gradient, the hybrid sheet reached its bending maximum. The maximum bending transformation and the stable surface thermal gradient were achieved at a very similar time scale.

As can be seen from the above discussion, our hybrid hydrogel sheet system is very dynamic under light irradiation. It coupled together heat transfer, mass (water) transport and macroscopic mechanical deformation. To provide a more fundamental understanding of our system, we conducted a coupled thermo-mechanical analysis using the thermodynamics of the PNIPAM hydrogel. The swelling behaviour of the PNIPAM hydrogel stemming from this microscopic mechanism can be captured by its thermodynamics:[30] the coil-to-globule transition is associated with a change in the macroscopic Helmholtz free energy. Moreover, the non-uniform swelling field in the hydrogel body is accompanied by interior stresses, as a result of the swelling difference between the hydrogel and its neighbouring material. In such a case, the total free energy of the hydrogel includes the strain energy in addition to the free energy due to the mixing of the PNIPAM network and water molecules. In the presence of a temperature gradient, the equilibrium responses of the PNIPAM hydrogel to the inhomogeneous temperature field are governed by a mechanical model which determines the steady states of the PNIPAM hydrogel as the Helmholtz free energy minima of the entire system (see the ESI†). The PNIPAM constitutive model is implemented in the ABAQUS user subroutine and the deformation is computed using the directly coupled thermo-mechanical analysis. Without missing the nature of the deformation, the exterior surfaces of the hydrogel sheet are set to be at infinite convection thermal exchange with the ambience in the heat transfer model. Here it was found that a localized stress field was established within the hybrid hydrogel sheet upon light irradiation (Fig. 4b). The hydrogel material in the exposed area underwent a gradual compression-to-stretch change due to the established thermal gradient, while the off-exposure areas remain a stress-free state (Fig. 4b). The asymmetry in the stress state in the hydrogel material actuated its bending. Further modelling studies show that the shape transformation of the hybrid hydrogel is robust for various boundary conditions and material properties (*e.g.*, finite convection and ambient temperature) (see Fig. S10–S15, ESI,† for details).

Our self-shaping hybrid hydrogel sheet represents a non-equilibrium dynamic system: it requires continuous energy supply (light energy) and energy dissipation (heat dissipation) to sustain its shape. The competition between the supply and dissipation of energy determines the behavior of the sheet's shape transformation. To study this, we used a striped light pattern to trigger the bending of the sheet (Fig. 5b). It was found that either the NIR laser power density or the irradiation stripe width should reach a certain threshold for the hybrid hydrogel sheet to bend (Fig. 5a). If the supplied light energy was low (small laser power density or small irradiation stripe width), the fast heat dissipation diminished the thermal gradient and disabled the bending of the sheet. The FEM study confirmed a positive correlation between the bending and the laser power density as well as the irradiation stripe width (Fig. 5c, d and Fig. S8, ESI†).

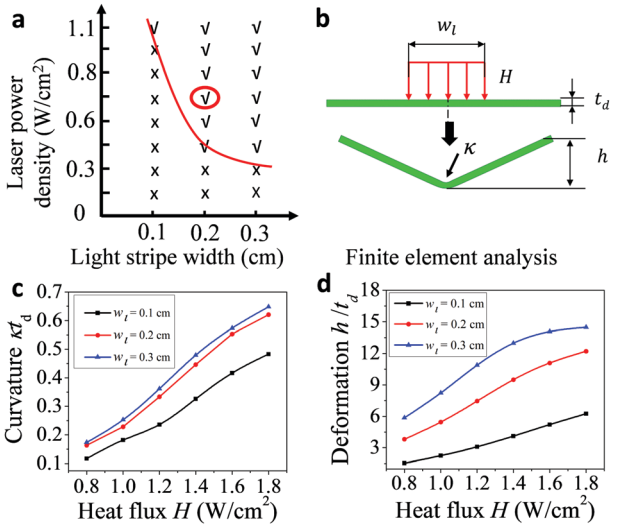

Fig. 5 (a) Experimental study on the bending of the hybrid hydrogel sheet as a function of laser power density and irradiation stripe width. The width of the rectangular irradiation stripe was varied while its length was kept as 0.9 cm. The red circle indicates the irradiation condition used in the current experiment. √: the sheet bent under the applied irradiation. X: the sheet exhibited no visible bending under the applied irradiation. (b–d) FEM analysis of the sheet's deflection (h/t_d) and bending curvature (κt_d) with respect to the laser power density and irradiation stripe width. The FEM results indicated that the deflection and bending curvature increased with the increase of either the laser power density or the irradiation stripe width.

It indicates that the bending increased with the increase of either the laser power density or the irradiation stripe width. Increasing the laser power density enhanced the heat generation. A larger thermal gradient was hence established in the sheet resulting in an increased bending. By increasing the irradiation stripe width, the thermal gradient was generated in a larger lateral area, which contributed to the increased bending.

In conclusion, we reported a simple and effective design of a 2-D macroporous hybrid hydrogel sheet that can transform into at least five different shapes (unlimited number in theory) under NIR light irradiation. Representative shapes achieved from the same 2-D hybrid sheet include helical, boat-like, hoof-like and saddle-like shapes. The transformation is highly reversible and ultrafast (on the order of seconds, while previous nonporous hydrogels of similar thickness transform on the order of minutes or even hours[25]). The hybrid sheet is composed of a thermo-responsive polymer, PNIPAM, and silver nanoparticles (AgNPs). Each shape transformation relies on the unique swelling pattern generated by the specific thermal gradient established upon light irradiation. The thermal gradient is created through a delicate balance between the continuous localized heating by the plasmonic AgNPs under NIR irradiation and the heat dissipation to the aqueous environment. We point out that accessible shape transformations of the hybrid hydrogel sheet rely on several factors, including: (i) size (aspect ratio; thickness) and shape of the original hydrogel sheet; (ii) laser irradiation pattern and its intensity; (iii) photothermal efficiency of the inorganic nanoparticles; (iv) mass and heat transport. We also highly expect that sequentially folding the same 2-D hydrogel material will further

greatly enrich the potential of its shape transformations.[31] In the sequential folding, a shape transformation is fixed before the next transformation is initiated. After the target shape is achieved, the hydrogel sheet can be restored to its original flat shape. Then a new type of transformation can be implemented to obtain a different shape. This sequential folding can potentially lead to a large array of on-demand shapes by reprogrammable origami of the same 2-D hydrogel material. The ultrafast, reprogrammable and NIR-light-responsive macroporous hybrid hydrogel sheet reported here represents an important step towards designing novel soft materials that can transform to adapt in an on-demand manner. The macroporous hybrid hydrogel sheet may find applications in artificial muscles, soft robotics, microfluidics, actuators, and biomedicine, *etc.* As an example, the composite hydrogel sheet can potentially serve as dynamic scaffolds for the generation of three-dimensional tissue-like structures. After the seeding and growth of arrays of single or multiple cells on the sheet, controlled exposure of the sheet to patterned NIR light drives the shape transformation of the cell arrays into tissue-like structures with defined geometries such as vascularized nerve tubes.[32] Moreover, such shape-transforming materials can be used as smart sensing wrappers. The sheet patterned with arrays of sensors can be triggered remotely to transform and conformably contact the lesion tissues with arbitrary shapes. The conformal contact between the tissue surface and sensors allows for sensing and mapping the local environment or disease biomarkers. The use of NIR light is beneficial for *in vivo* application, owing to its large penetration depth and minimal damage to soft tissues.

Acknowledgements

Z. N. gratefully acknowledges the financial support of the National Science Foundation (grants: DMR-1255377, CHE-1505839), 3M Non-tenured Faculty Award and Startup fund from the University of Maryland. T. L. and Z. J. are grateful for the support of NASA (Grant number: NNX12AM02G). We also acknowledge the support of the Maryland NanoCenter and its NispLab. The NispLab is supported in part by the NSF as a MRSEC Shared Experimental Facilities.

Notes and references

1 E. Sharon, M. Marder and H. L. Swinney, *Am. Sci.*, 2004, **92**, 254–261.
2 M. J. Harrington, K. Razghandi, F. Ditsch, L. Guiducci, M. Rueggeberg, J. W. C. Dunlop, P. Fratzl, C. Neinhuis and I. Burgert, *Nat. Commun.*, 2011, **2**, 337.
3 S. J. Gerbode, J. R. Puzey, A. G. McCormick and L. Mahadevan, *Science*, 2012, **337**, 1087–1091.
4 Y. Forterre, J. M. Skotheim, J. Dumais and L. Mahadevan, *Nature*, 2005, **433**, 421–425.
5 R. Kempaiah and Z. H. Nie, *J. Mater. Chem. B*, 2014, **2**, 2357–2368.
6 L. Ionov, *Adv. Funct. Mater.*, 2013, **23**, 4555–4570.
7 L. Ionov, *Mater. Today*, 2014, **17**, 494–503.
8 D. H. Gracias, *Curr. Opin. Chem. Eng.*, 2013, **2**, 112–119.
9 S. H. Jiang, F. Y. Liu, A. Lerch, L. Ionov and S. Agarwal, *Adv. Mater.*, 2015, **27**, 4865–4870.
10 E. Wang, M. S. Desai and S. W. Lee, *Nano Lett.*, 2013, **13**, 2826–2830.
11 G. Stoychev, N. Puretskiy and L. Ionov, *Soft Matter*, 2011, **7**, 3277–3279.
12 Z. J. Wei, Z. Jia, J. M. Athas, C. Y. Wang, S. R. Raghavan, T. Li and Z. H. Nie, *Soft Matter*, 2014, **10**, 8157–8162.
13 J. Deng, J. F. Li, P. N. Chen, X. Fang, X. M. Sun, Y. S. Jiang, W. Weng, B. J. Wang and H. S. Peng, *J. Am. Chem. Soc.*, 2016, **138**, 225–230.
14 Y. Hu, G. Wu, T. Lan, J. J. Zhao, Y. Liu and W. Chen, *Adv. Mater.*, 2015, **27**, 7867–7873.
15 S. Iamsaard, S. J. Asshoff, B. Matt, T. Kudernac, J. Cornelissen, S. P. Fletcher and N. Katsonis, *Nat. Chem.*, 2014, **6**, 229–235.
16 A. W. Hauser, D. Q. Liu, K. C. Bryson, R. C. Hayward and D. J. Broer, *Macromolecules*, 2016, **49**, 1575–1581.
17 Y. Yang, Z. Q. Pei, Z. Li, Y. Wei and Y. Ji, *J. Am. Chem. Soc.*, 2016, **138**, 2118–2121.
18 Z. Zhu, E. Senses, P. Akcora and S. A. Sukhishvili, *ACS Nano*, 2012, **6**, 3152–3162.
19 Y. L. Tai, G. Lubineau and Z. G. Yang, *Adv. Mater.*, 2016, **28**, 4665–4670.
20 M. D. Norman, J. Finn and T. Tregenza, *Proc. R. Soc. B*, 2001, **268**, 1755–1758.
21 J. Kim, J. A. Hanna, M. Byun, C. D. Santangelo and R. C. Hayward, *Science*, 2012, **335**, 1201–1205.
22 J. H. Na, A. A. Evans, J. Bae, M. C. Chiappelli, C. D. Santangelo, R. J. Lang, T. C. Hull and R. C. Hayward, *Adv. Mater.*, 2015, **27**, 79–85.
23 G. Stoychev, S. Zakharchenko, S. Turcaud, J. W. C. Dunlop and L. Ionov, *ACS Nano*, 2012, **6**, 3925–3934.
24 Z. L. Wu, M. Moshe, J. Greener, H. Therien-Aubin, Z. H. Nie, E. Sharon and E. Kumacheva, *Nat. Commun.*, 2013, **4**, 1586.
25 H. Therien-Aubin, Z. L. Wu, Z. H. Nie and E. Kumacheva, *J. Am. Chem. Soc.*, 2013, **135**, 4834–4839.
26 A. W. Hauser, A. A. Evans, J. H. Na and R. C. Hayward, *Angew. Chem., Int. Ed.*, 2015, **54**, 5434–5437.
27 X. Z. Zhang, Y. Y. Yang, T. S. Chung and K. X. Ma, *Langmuir*, 2001, **17**, 6094–6099.
28 T. Binkert, J. Oberreich, M. Meewes, R. Nyffenegger and J. Ricka, *Macromolecules*, 1991, **24**, 5806–5810.
29 M. Shibayama, T. Tanaka and C. C. Han, *J. Chem. Phys.*, 1992, 97.
30 F. Afroze, E. Nies and H. Berghmans, *J. Mol. Struct.*, 2000, **554**, 55–68.
31 E. Palleau, D. Morales, M. D. Dickey and O. D. Velev, *Nat. Commun.*, 2013, **4**, 2257.
32 B. Yuan, Y. Jin, Y. Sun, D. Wang, J. S. Sun, Z. Wang, W. Zhang and X. Y. Jiang, *Adv. Mater.*, 2012, **24**, 890–896.